Bull. Disas. Prev. Res. Inst., Kyoto Univ., Vol. 19, Part 3, No. 162, February, 1970

Shear Strength of Sand under a Vibrating Load

By Toru SHIBATA and Hiroshi YUKITOMO

(Manuscript received October 31, 1969)

Abstract

This paper presents some test results on the strength of saturated and dry sands under drained triaxial vibratory loading conditions. In these tests the loadings are controlled so that the values of τ_d/σ_{Nd}' are in accord with the angle of mobilized internal friction, ϕ_{mo}', where τ_d is the dynamic shearing stress on the shear plane and σ_{Nd}' is the dynamic normal stress.

The triaxial vibrating tests are carried out under the following loading conditions: the amplitudes of lateral confining pressures are kept constant at 0.1, 0.2, 0.3, and 1.0 kg/cm², and the amplitude of axial pressure is controlled so that the angle between the normal stress and the resultant vibrating stress is in accord with ϕ_{mo}'.

The comparisons between the test results on saturated sands under drained triaxial vibratory loading conditions and those of static triaxial compression tests are made. The dynamic strength of sands depends on various factors, and tentative conclusions obtained are as follows. (1) The internal frictions in terms of the effective stress of sand under the vibratory loading conditions decrease with the increasing of the amplitude of lateral confining pressure and the frequency of vibration. (2) The strength of sand under vibration decreases with the increasing of the initial void ratio but this tendency of strength-loss is not observed for the larger pressure amplitude.

1. Introduction

The dynamic characteristics of soils under a vibrating load are usually different from the static one. In general quicker loading or a higher frequency produces larger coefficients of elasticity and strength of soils. The dynamic tests of soils consist of two kinds of test: transient and vibratory tests. Moreover the latter test consists of vibratory loading and loading test during vibration.

In the conventional triaxial loading test during vibration, one of the axial or lateral confining pressures is changed periodically, and consequently, the value of τ_d/σ_{Nd}' is not equal to tan ϕ_{mo}', where τ_d is the dynamic shear stress, σ_{Nd}' is the dynamic normal stress on the shear plane and ϕ_{mo}' is the mobilized angle of internal friction. This means that, if an example is given by the mutual forces produced by live- and dead-loads, the direction of the resultant force on the shear plane by the live load does not coincide with that of the dead load. In such a case it is difficult to chose a suitable failure criterion during vibrational shearing.

In this paper, therefore, both of the periodic axial and lateral confining pressures are controlled dependently so as to follow the relation of $\tau_d/\sigma_{Nd}' = \tan\phi_{mo}'$. If this relation between τ_d/σ_{Nd}' and tan ϕ_{mo}' is maintained during shear, the dynamic strength of sand may easily be determined by the failure criterion of

the maximum principal stress ratio.

2. Testing Procedure

(1) Stress states in the triaxial vibrating tests

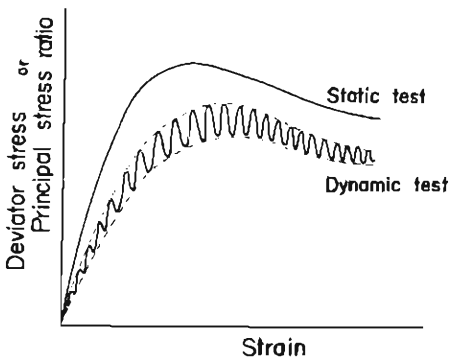

Fig. 1 Schematic expressions of stress vs. strain curves for both static and dynamic shear tests.

Up to now the conventional triaxial vibrating tests[1~4] have been carried out by periodically changing one of the axial or lateral confining pressures. In these cases the direction angle of the resultant vibrating stress does not coincide with the angle of mobilized internal friction, and the stress vs. strain curve may be obtained as shown schematically in Fig. 1. From the stress vs. strain curve in Fig. 1., it is difficult to determine the unique dynamic shear strength of soils.

Fig. 2 shows the stress states of the soil element in the various types of triaxial tests. In column (I) are shown the combinations of the principal stresses and their vibrational amplitudes, where $(\sigma_1-\sigma_3)_d$ and σ_{3d} are the stress amplitudes of deviator and lateral stresses, respectively. In this figure the

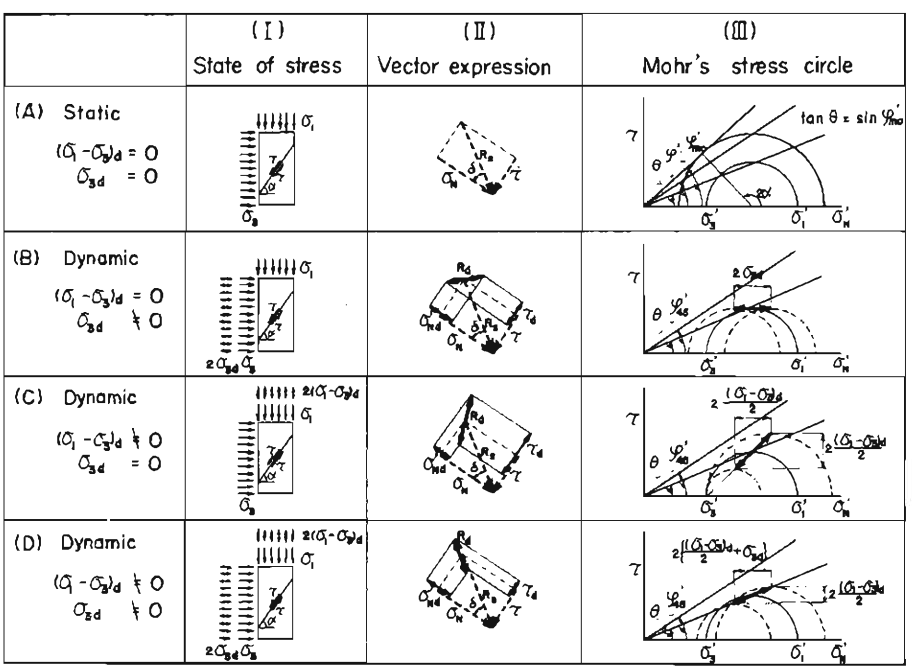

Fig. 2 Various types of stress states produced by the triaxial tests.

stress states are classified into the following four types:

(A) $(\sigma_1-\sigma_3)_d=0$; $\sigma_{3d}=0$,
(B) $(\sigma_1-\sigma_3)_d=0$; $\sigma_{3d}\neq 0$,
(C) $(\sigma_1-\sigma_3)_d\neq 0$; $\sigma_{3d}=0$ and
(D) $(\sigma_1-\sigma_3)_d\neq 0$; $\sigma_{3d}\neq 0$.

Type (A) corresponds to the static triaxial test and types (B) and (C) to the conventional vibrational triaxial tests. The stress state which is produced by the test in this paper is type (D).

In column (II) in Fig. 2 are shown the stress-vectors on the shear plane: the vector R_s represents the static resultant stress induced by the static principal stresses, and the vector R_s represents the dynamic or amplitude of the resultant stress. δ is the angle between the direction of R_s and the normal stress on the shear plane. It is noted from this figure that for type (D) the angle between the direction of R_d and the dynamic normal stress σ_{Nd}' coincides with δ.

In column (III) in Fig. 2 are shown Mohr's stress circles for four types of stress states. The thick-solid arrows express the directions and amounts of the resultant vibrating stresses. Angle θ is concerned with the angle of mobilized internal friction ϕ_{mo}' as $\tan\theta=\sin\phi_{mo}'$. As described above, (B) corresponds to a type of stress state produced by the test in which only the confining pressure is periodically changed. The direction of resultant vibrating stress is therefore in parallel with the σ_N'-axis. Type (C) is produced by the test in which only the axial pressure is periodically changed, and the direction of the resultant vibrating stress makes an angle of 45° to the σ_N'-axis. In both cases, (B) and (C), the directions of the resultant vibrating stresses are not in accord with the angle of mobilized internal friction ϕ_{mo}', and therefore it is rather difficult to decide the dynamic failure line. On the other hand, in type (D) the inclination of the resultant stress during vibrational shear coincides with the angle of mobilized internal friction ϕ_{mo}' and unique failure line may be obtained.

(2) Controlling of applied stresses

In this investigation dynamic tests of sands were carried out in the stress state as shown in Fig. 2 (D). In order to obtain such a stress state, it is

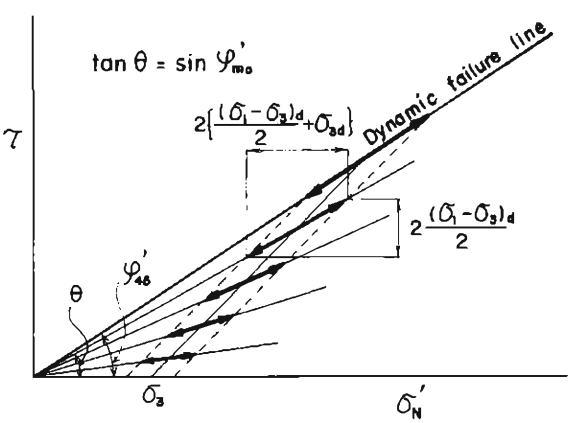

Fig. 3 Change of vibrational resultant stress.

necessary to satisfy the following relationship between the applied stresses:—

$$\frac{(\sigma_1-\sigma_3)}{\sigma_3}=\frac{(\sigma_1-\sigma_3)_d}{\sigma_{3d}},$$

where $(\sigma_1-\sigma_3)_d$ is the amplitude of deviator stress and σ_{3d} is the amplitude of confining pressure.

The actual tests were performed by increasing $(\sigma_1-\sigma_3)$ under the condition of constant values of σ_3 and σ_{3d}, provided that $(\sigma_1-\sigma_3)_d$ was controlled to follow the above relationship.

Fig. 3 shows the path of the resultant stresses during shear on the τ vs. σ_N' diagram. In this figure the thick-solid arrow expresses the direction and magnitude of the resultant vibrating stress; their directions coincide with the lines through origin and their angles of inclination increase gradually. Consequently if the stress vs. strain curves were drawn on the basis of the principal stress ratio, (σ_1'/σ_3') vs. strain, a smooth curve may be obtained as will be seen in Figs. 6, 8, and 11. Moreover, in the drained test the failure criterion of $(\sigma_1'/\sigma_3')_{max}$ coincides with that of $(\sigma_1-\sigma_3)_{max}$ and it is easy to determine the dynamic strength of soils.

3. Testing Apparatus and Sample

(1) *Apparatus*

A diagrammatic layout of apparatus is given in Fig. 4. A bellows is inserted in place of the proving-ring of conventional triaxial apparatus, and the water pressure from a vibrating pressure generator is added to the static pressures in the bellows and the triaxial cell. The vibrating pressure generator is composed of two cam cylinders and two bellows, and the mechanical up-and-down motion

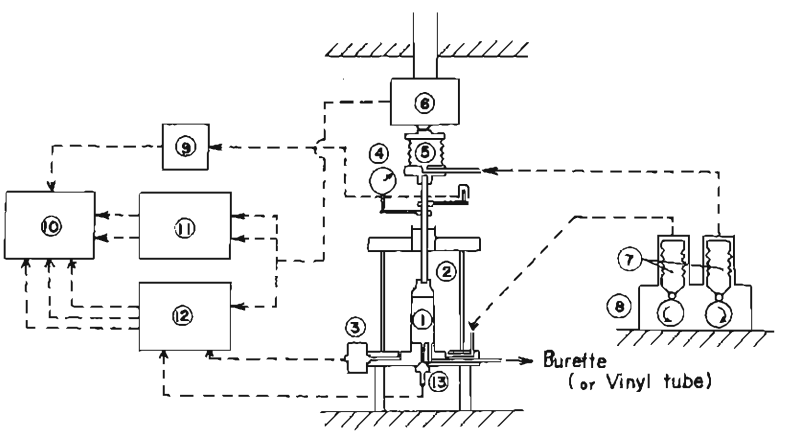

Fig. 4 Layout of the new type vibrational triaxial apparatus.

is changed into water pressure through the bellows in contact with each other. Consequently vibrating pressure can be added independently to the static axial and lateral pressures. Moreover, the pressure amplitude and frequency of vibration can be increased or decreased continuously over a wide range. The shape of the pulse is a trocoid which is similar to a sinusoidal wave. The phase difference between the axial and lateral vibrating pressures can be changed by the gear fixed to the cam.

The loading in the tests is of the controlled deformation type. The axial pressure and its amplitude are recorded by an electro-magnetic oscillograph through a load cell and a dynamic strain meter. The lateral confining pressure and its amplitude are also recorded by the electro-magnetic oscillograph through a pressure head and a dynamic strain meter. The mean value of the axial deformation of the specimen is measured by a dial gage, but the amplitude of deformation at the upper end of the specimen is recorded by the electro-magnetic oscillograph through a differential displacement-meter. The amount of volume change is measured by a burette in the case of saturated sand, or a thin vinyl tube in the case of dry sand. The pore pressure measurement of saturated or dry sand is made in order to ascertain that there is no residual pressure.

(2) Sample

The samples used in these tests are saturated and dry River sand, and dry Toyoura sand. All series of tests were performed on specimens having a diameter of 3.5 cm and a height of about 8.0 cm. The specific gravity of samples are 2.66 (River sand) and 2.64 (Toyoura sand). Their minimum and maximum void ratios are 0.51-0.80 (River sand) and 0.64-0.95 (Toyoura sand) respectively. The grain size distribution curves of their samples are shown in Fig. 5.

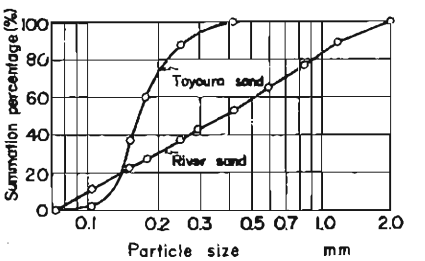

Fig. 5 Grain size distributions of the samples.

4. Test Results and Discussions

The dynamic strength of sands may be influenced by many factors, but the following three factors will be considered in this paper; the amplitude of lateral confining pressure, the initial void ratio of sand and the frequency or acceleration of vibrations.

(1) Amplitude of confining pressure

A series of drained vibrating triaxial tests were carried out on the saturated River sand for various values of confining pressures, $\sigma_3 = 1.0$, 1.5, 2.0 kg/cm^2, and amplitudes of confining pressures, $\sigma_{3d} = 0$, 0.1, 0.2, 0.3 kg/cm^2. The frequency of vibration was 5.0 cps for all tests.

Some examples of stress vs. strain and volume vs. strain curves are shown in Fig. 6. In this case the effective principal stress ratio (σ_1'/σ_3') is used for the vertical axis and therefore smooth stress vs. strain curves are obtained

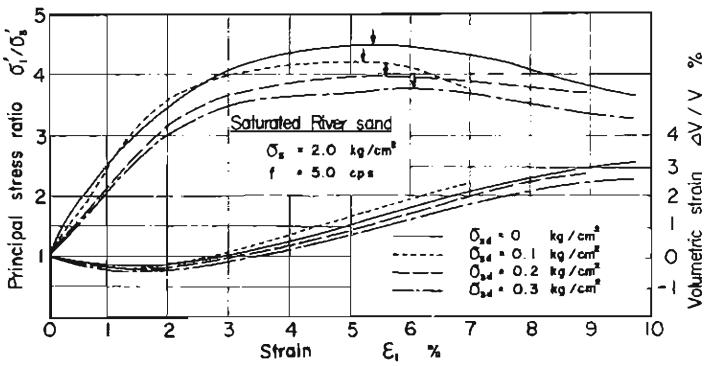

Fig. 6 Examples of stress vs. strain and volumetric strain vs. axial strain curves.

during the vibrational shearing test. And the value of the maximum principal stress ratio $(\sigma_1'/\sigma_3')_{max}$ may be obtained as shown by the arrow in Fig. 6. From this figure it is seen that the value of $(\sigma_1'/\sigma_3')_{max}$ decreases with the increasing of the amplitude of confining pressure σ_{3d} for the same value of σ_3.

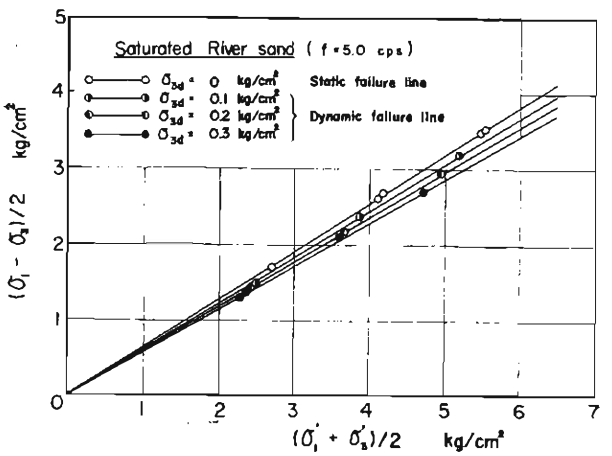

Fig. 7 Failure lines for various values of σ_{3d}.

The deviator stresses corresponding to $(\sigma_1'/\sigma_3')_{max}$ obtained from Fig. 6 are plotted for $(\sigma_1'+\sigma_3')/2$ at failure in Fig. 7. It is obvious that the straight lines through origin are obtained for each amplitude of confining pressure σ_{3d} and that the slope of these lines, viz. the angle of internal friction ϕ', decreases with the increasing of σ_{3d}.

As mentioned above, no variation of the angle of internal friction was observed for the same value of σ_{3d} and then the variation of ϕ' with σ_{3d} will be tested as follows. Fig. 8 shows some examples of the effective stress ratio (σ_1'/σ_3') vs. strain and the volumetric strain $(\Delta V/V)$ vs. axial strain curves obtained for the various values of void ratio and of σ_{3d}. In this figure, for $\sigma_{3d}=0$ and 0.3 kg/cm² ΔV is slightly contractive (a negative sign) at the initial small

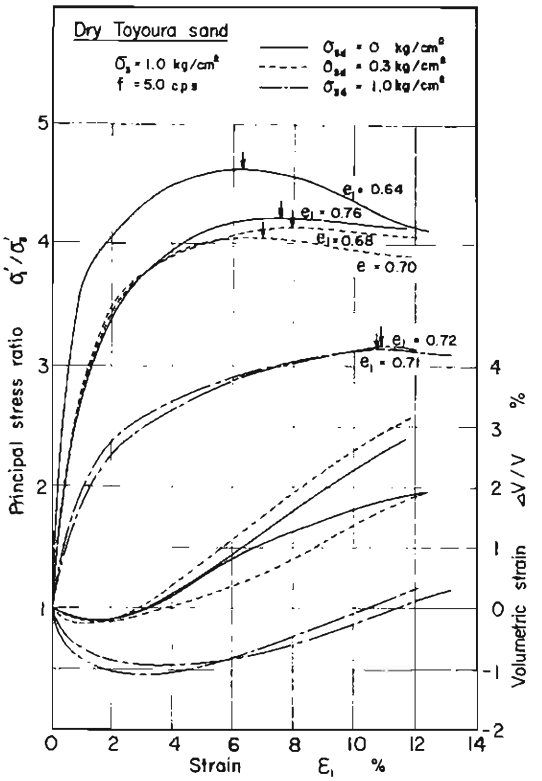

Fig. 8 Examples of stress vs. strain and volumetric strain vs. axial strain curves.

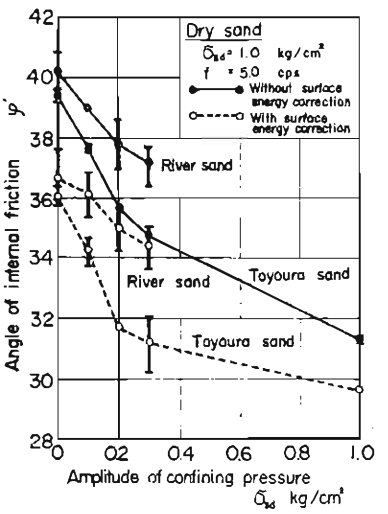

Fig. 9 Decreases of the angle of internal frictions with the amplitudes of confining pressure.

strain, but thereafter it expands (a positive sign). From a habitual point of view, therefore, it may be meant to have been sheared in a dense condition less than the critical void ratio. On the other hand, for $\sigma_{3d}=1.0$ kg/cm² the volume change equals zero at the time of $(\sigma_1'/\sigma_3')_{max}$, and it is presumed that the critical void ratio is about 0.7. However in a drained triaxial test under constant confining pressure, the mean effective principal stress σ_m' increases with the shear stress and it is necessary to measure the volume change due to the increasing of σ_m' in order to discuss the critical void ratio of sand during vibrations more precisely. In this connection, an other paper by the authors will be published in the near future.

In Fig. 9 the internal frictions ϕ' of both samples, River and Toyoura sands, are plotted for the amplitude of lateral confining pressure σ_{3d}. In this figure the dotted lines show a result with surface energy correction by Bishop's method. From Fig. 9 it is seen that ϕ' decreases considerably with the increasing of σ_{3d}; values of ϕ' smaller than the statically measured value by 6-8 degrees are obtained.

In this paper the decreasing of strength under vibration is considered on the basis of the amplitude of confining pressure σ_{3d}, but as explained in Fig. 3 the

magnitude of the vibrating resultant stress increases with the progress of shearing, and therefore it should be borne in mind that σ_{3d} is merely a convenient parameter.

(2) Void ratio of sand

It is well known that the angle of internal friction is remarkably affected by the magnitude of void ratio.[5,6,7] Moreover it is proved that the dynamic characteristics of soils, for example the liquefaction of sand, depend on the density. In order to investigate the influence of density on the dynamic strength of sand, in this paper, a series of tests are performed on specimens having various initial void ratios with a range of 0.64-0.86.

Fig. 10 shows the relationships between $(\sigma_1'/\sigma_3')_{max}$ and initial void ratio for three kinds of σ_{3d}; 0, 0.3 and 1.0 kg/cm². The results with surface energy correction are shown by the dotted lines. From this figure it will be seen that the rate of strength-loss related to the initial void ratio (the slope of the line) depends on the magnitude of pressure amplitude σ_{3d}, and that the rate of strength-loss decreases with increases of σ_{3d}: but in the case of a large amplitude of confining pressure no difference of strength for different initial void ratio is observed. One of the causes of this phenomenon may be the difference of amount of volume change with the initial void ratio.

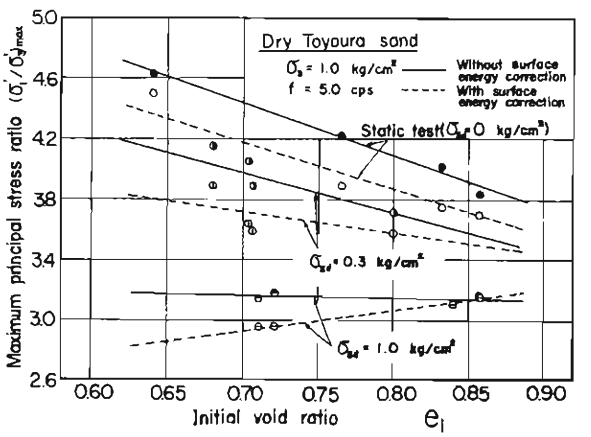

Fig. 10 Influence of the initial void ratio on the strength of sand for various values of σ_{3d}.

Fig. 11 shows a comparison of volume change $\Delta V/V$ with the initial void ratio. In the case of $e_i \approx 0.71$, $\Delta V/V = 0$ at failure, but in the case of $e_i \approx 0.85$, $\Delta V/V = -2 \sim 3.5\%$ (contraction) at failure. This means that if the larger pressure amplitude of vibration is applied on the specimens each of them having smaller or larger initial void ratios has almost the same void ratio at failure and that their strengths show very closed values.

The above-mentioned are the results of tests under drained conditions. If no dissipation of excess pore pressure occurs on account of quick loading, the liquefaction of loose sand may be caused due to the strength decreasing.

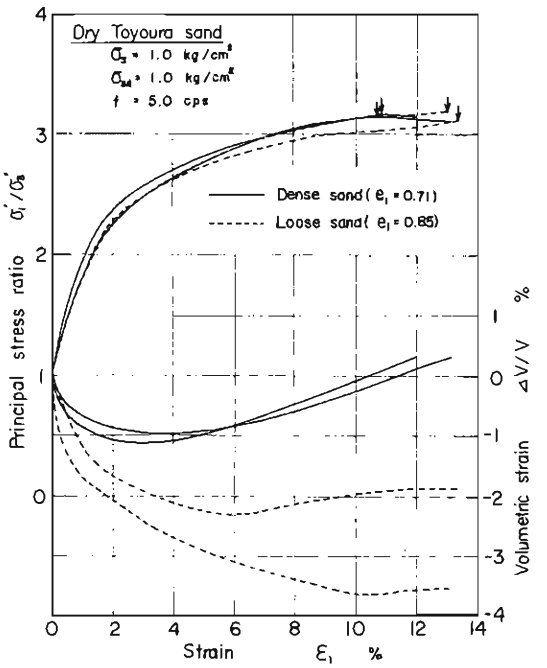

Fig. 11 Examples of stress vs. strain and volumetric strain vs. axial strain curves.

(3) *Frequency and acceleration of vibrations*

In order to elucidate the strength of sand during vibration, it seems to be necessary to clarify the influences of frequency and acceleration on the strength. In this article, the results of tests on dry Toyoura sand having various initial void ratios under three kinds of frequency f less than the resonance one, f=0.6, 5.0 and 12.2 cps, will be discussed.

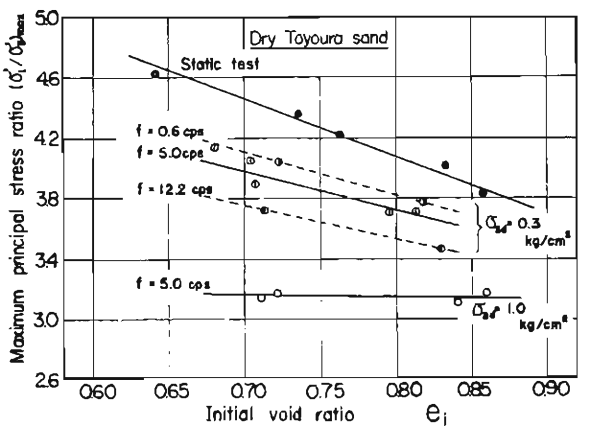

Fig. 12 Influence of the initial void ratio on the strength of sand for various values of frequency f.

In Fig. 12 the maximum principal stress ratios $(\sigma_1'/\sigma_3')_{max}$ are plotted for the initial void ratio for each value of frequency. In this figure if the results for the same amplitude of confining pressure are noticed, e. g. $\sigma_{3d}=0.3$ kg/cm^2, the strength will decrease with increasing of frequency for the same values of initial void ratio. Seed and Lundgren[8] have shown that there was a possibility of excess pore water pressure remaining in the drained quick loading test on sand having a large permeability. If some residual excess pore pressure exists at a high frequency of vibration, therefore, its effect on the strength should be taken into consideration. In the authors' tests, however, the indication of the pore pressure gage was almost zero at the higher frequency of 12.2 cps.

The accelerations of vibration estimated on the basis of the measured amplitudes of deformation at the upper end of specimens are plotted for the axial strain in Fig. 13. As will be seen from this figure, the maximum acceleration of vibration is of the order of $10^{-2}g$ and the effect of it on the strength is not so remarkable. Moreover the difference of acceleration during shear is also not so remarkable. But if the case of $\sigma_{3d}=0.3$ kg/cm^2 is considered, the acceleration increases with the frequency, and it does not contradict the tendency of the decreasing of the strength with the higher frequency as shown in Fig. 12.

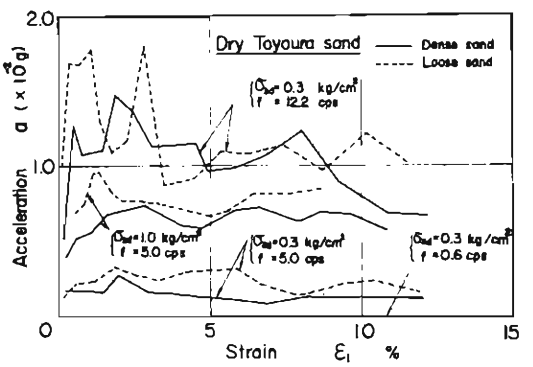

Fig. 13 Change of the acceleration of vibration with axial strain.

5. Conclusion

Some test results on the strength of sands under drained triaxial vibratory loading conditions were presented, and comparisons between the strengths of dynamic and static loading conditions were also made. In these tests the loadings were controlled so that the value of τ_d/σ_{Nd}' was in accord with the angle of mobilized internal friction ϕ_{mo}'. The dynamic strength of sands depends on various factors, and tentative conclusions obtained here are as follows:—

(1) The angle of internal friction of sand ϕ' decreased with the increasing of σ_{3d}, the amplitude of lateral confining pressure. Almost the same tendency of this strength-loss was observed irrespective of the surface energy corrections. The observed accelerations of vibration at the upper end of the specimen were of the order of $10^{-2}g$, and the effect of it on the strength of sand did not seem to be so remarkable. Nevertheless the ϕ'-values during vibration at $\sigma_{3d}=1.0$

kg/cm², for example, decreased about 6-8 degrees from the static one. Moreover the the influence of the frequency of vibration on the strength of sand was rather remarkable: the higher the frequency became the lower the strength was.

(2) In general dynamic strength increases with the increasing of the density of sand, but this densification-effect of sand on the strength may not be expected for the larger external dynamic force. For example, in the case of a large amplitude of confining pressure, $\sigma_{3d}=1.0$ kg/cm², no difference of strength for the different initial void ratio was observed. One of the causes of this phenomenon may be the difference of the amount of volume change with the initial density of sand.

Acknowledgment

The writers are indebted to Professor S. Murayama for constructive suggestions during the development of the test equipment.

References

1) Murayama, S. and T. Shibata : On the Dynamic Properties of Clay, Proc. 2nd World Conf. on Earthquake Eng., 1960, p. 297.
2) Folque, J. : Dynamic Triaxial Tests of Compacted Unsaturated Soils, Proc. 6th Int. Conf. S. M. F. E., 1965, p. 217.
3) Olson, R. E. and H. Kane : Dynamic Shearing Properties of Compacted Clay at High Pressure, Proc. 6th Int. Conf. S. M. F. E., Vol. 1, 1965, p. 328.
4) Timmerman, D. H. and T. H. Wu : Behavior of Dry Sands under Cyclic Loading, Proc. A. S. C. E., SM 4, 1969, p. 1097.
5) Bjerrum, L., S. Kringstad, and O. Kummeneje : The Shear Strength of Fine Sand, Proc. 5th Int. Conf. S. M. F. E., Vol. 1, 1961, p. 29.
6) Bishop, A. W. and A. K. G. Eldin : The Effect of Stress History on the Relation between ϕ' and Porosity in Sand, Proc. 3rd Int. Conf. S. M. F. E., Vol. 1, 1958, p. 1.
7) Cornforth, D. H. : Some Experiments on the Influence of Strain Conditions on the Strength of Sand, Géotechnique, Vol. 14, 1964, p. 143.
8) Seed, H. B. and R. Lundgren : Investigation of the Effect of Transient Loading on the Strength and Deformation Characteristics of Saturated Sand, Proc. A. S. T. M., Vol. 54, 1954, p. 1288.